Earthquakes and Structures, *Vol. 17, No. 6 (2019) 545-556*
DOI: https://doi.org/10.12989/eas.2019.17.6.545

Experimental and numerical investigation of the seismic performance of railway piers with increasing longitudinal steel in plastic hinge area

Jinhua Lu[1], Xingchong Chen[1], Mingbo Ding*[1,2], Xiyin Zhang[1], Zhengnan Liu[1] and Hao Yuan[1]

[1]*School of Civil Engineering, Lanzhou Jiaotong University, Lanzhou, Gansu 730070, China*
[2]*Key Laboratory of Road and Bridge and Underground Engineering of Gansu Province, Lanzhou Jiaotong University, Lanzhou, Gansu 730070, China*

(*Received May 29, 2019, Revised July 31, 2019, Accepted October 22, 2019*)

Abstract. Bridge piers with bending failure mode are seriously damaged only in the area of plastic hinge length in earthquakes. For this situation, a modified method for the layout of longitudinal reinforcement is presented, i.e., the number of longitudinal reinforcement is increased in the area of plastic hinge length at the bottom of piers. The quasi-static test of three scaled model piers is carried out to investigate the local longitudinal reinforcement at the bottom of the pier on the seismic performance of the pier. One of the piers is modified by increased longitudinal reinforcement at the bottom of the pier and the other two are comparative piers. The results show that the pier failure with increased longitudinal bars at the bottom is mainly concentrated at the bottom of the pier, and the vulnerable position does not transfer. The hysteretic loop curve of the pier is fuller. The bearing capacity and energy dissipation capacity is obviously improved. The bond-slip displacement between steel bar and concrete decreases slightly. The finite element simulations have been carried out by using ANSYS, and the results indicate that the seismic performance of piers with only increasing the number of steel bars (less than65%) in the plastic hinge zone can be basically equivalent to that of piers that the number of steel bars in all sections is the same as that in plastic hinge zone.

Keywords: increased longitudinal reinforcement; railway bridge piers; quasi-static test; seismic performance

1. Introduction

Pier, which transfers vertical load and bears horizontal load, is a very important element of bridge structures (Ohno and Nishioka 1984, Iacobucci *et al.* 2003, Xue *et al.* 2018). In the investigation of earthquake disasters occurred, it is found that bridge piers are more vulnerable in bridge structures under the action of earthquake load (PC 1995, Bruneau *et al.* 1996, Kuochun *et al.* 2000). Once the pier fails during the earthquake, the entire bridge structure will suffer severe damage, what's worse, it can even result in collapse, causing casualties and major economic losses (Tehrani and Mitchell 2013, Abdelnaby *et al.* 2014). Therefore, it is particularly important to ensure the seismic performance of bridge piers for the safety of bridge structures.

Since the 1960s, the seismic performance of reinforced concrete piers has been studied in the United States, New Zealand, Japan and other countries. Jaradat *et al.* (1998, 1999) studied the seismic performance of six circular section piers built before 1970s under cycle loading. The results showed that the shear span ratio, longitudinal reinforcement ratio and stirrup ratio had great influence on the seismic performance of piers and the lap length of longitudinal reinforcement has little effect on bending bearing capacity. In the study of RC piers with different stirrups ratio, Rajput and Sharma (2018) found that increasing the ratio of stirrups could improve the ductility of piers. Subsequently, some parameters affecting the seismic performance of RC piers were studied by researchers from different countries (Tanaka 1990, Wehbe *et al.* 1999, Lehman *et al.* 2004, Xiao and Zhang 2008, Ding *et al.* 2018). Based on the summary of these previous studies, it has been found that the critical factors affecting the seismic performance of RC piers are axial compression ratio, shear span ratio, stirrup ratio, concrete strength and longitudinal reinforcement ratio, etc. Mander *et al.* (1988, 1996) and Kunnath *et al.* (1997) carried out a further study on reinforced concrete piers and obtained the constitutive model of confined concrete suitable for circular and rectangular RC piers. Because the influence of the reinforcement ratio on the seismic performance of the pier is more critical, this parameter has attracted the attention of many researchers. Jiang *et al.* (2013) carried out quasi-static tests on high-speed railway piers with longitudinal reinforcement ratios of 0.15%, 0.45% and 0.75%. It has been found that with the increase of the reinforcement ratio, the hysteresis curve of the pier becomes fuller and more energy is dissipated, meanwhile, the stiffness and bearing capacity of piers are increasing. Obviously, increasing the pier reinforcement ratio can effectively improve its seismic performance. In addition, the same viewpoint has been also found in the studies of Iwasaki *et al.* (1985), Priestley and Benzoni (1996), Meli *et al.* (1984), Panagiotis (Mergos and Kappos 2015), Zhao *et al.* (2014), Su *et al.* (2017) and so on.

In the existing research, the longitudinal reinforcement

*Corresponding author, Professor
E-mail: ding_mingbo@126.com

http://www.techno-press.com/journals/easandsubpage=7
ISSN: 2092-7614 (Print), 2092-7622 (Online)

Fig. 1 Damage of the piers with bending failure

ratio of all sections of the pier is exactly the same. However,in the investigations of Wenchuan Earthquake (Jia *et al.* 2015), Yushu Earthquake (Ni *et al.* 2010) and Jiuzhaigou Earthquake (Wang *et al.* 2017) and other large earthquakes, it has found that the seriously damaged part of the pier with bending failure is mainly concentrated on the range of the plastic hinge length at the bottom of the pier. There is no serious damage such as concrete crushing or peeling off above the length of plastic hinge (Fig. 1) (Sun 2012). The longitudinal reinforcement above the plastic hinge length of the bridge pier hardly functions, resulting in the waste of steel bars. In building structures, the lap splice increases the longitudinal reinforcement ratio at the bottom of columns. Aboutaha (Aboutaha *et al.* 1996, Aboutaha *et al.* 1999) studied the column with the lap splice of the longitudinal steel bars and found that the seismic performance of this kind of column was insufficient. These papers have presented the reasons for the insufficient seismic performance of columns: inadequate confined in the lap splice length range of longitudinal steel bars. Similar problems have been found in subsequent studies and the columns are prone to failure at the lap splice location of reinforcing bars (Valluvan *et al.* 1993, Harries *et al.* 2006, Ghosh and Sheikh 2007, Lee and Han 2019). This method of the lap splice of longitudinal reinforcement is not suitable for bridge piers, but it can be used for reference in the arrangement of longitudinal reinforcement of bridge piers.

This study proposes a new arrangement method of longitudinal reinforcement for railway piers with bending failure with low longitudinal steel bars ratio, i.e., the number of longitudinal reinforcement bars is increased only in the plastic hinge region, while the number of longitudinal reinforcement bars above the plastic hinge region remains unchanged. In this way, the longitudinal reinforcement ratio of the section of the plastic hinge zone at the bottom of the pier is increased under the condition of insignificant increase of the total amount of reinforcing steel bars. At the same time, the bridge pier is ensured to have sufficient constraint in the plastic hinge area. A large-scale specimen with increasing number of longitudinal reinforcement in the plastic hinge area and two comparative large-scale specimens have been tested to verify the feasibility of this method to improve the seismic performance of bridge piers.

2. Specimen preparation

2.1 Determination of increased longitudinal reinforcement height

Based on the investigation of different earthquake damages, the damage of bridge piers with bending failure is mainly concentrated on the plastic hinge area at the bottom of pier, and the calculation method of plastic hinge length is also stipulated in accordance with national codes.

The length of plastic hinge (L_p) is calculated using Eq. (1) of China code (China 2008), and the minimum value of the calculation results are adopted.

$$L_P = \begin{cases} 0.08L+0.022d_s f_y \geq 0.044d_s f_y \\ \dfrac{2}{3}b \end{cases} \tag{1}$$

Where L is pier height; b is the short edge of the rectangular section pier or the diameter of circular section pier; d_s is the diameter of longitudinal ribs; f_y is the standard value of tensile strength of longitudinal reinforcement.

L_p is calculated using Eq. (2) of Caltrans code (Caltrans 2006).

$$L_P = 0.08L+0.022d_s f_{ye} \geq 0.044d_s f_{ye} \tag{2}$$

Where f_{ye} is the yield strength of longitudinal reinforcement.

L_p is calculated using Eq. (3) of AASHTO code (AASHTO 1995).

$$L_P = 0.08L+9d_s \tag{3}$$

L_p is calculated using Eq. (4) of Eurocode 8 code (8 2005), and the minimum value of the calculation results is selected.

$$\left. \begin{aligned} L_P &= 0.1L+0.015d_s f_{ye} \\ L_P &= \left(0.4 \sim 0.6\right)H \end{aligned} \right\} \tag{4}$$

Where H is the width of section in the loading direction, or the diameter of circular section pier.

L_p is calculated using Eq. (5) of Japan code “JRA” (Association 1996), and the minimum value of the calculation results is applied.

$$\left. \begin{aligned} L_P &= 0.2L - 0.1H \\ 0.1H &\leq L_P \leq 0.5H \end{aligned} \right\} \tag{5}$$

National standards differ in the calculation of plastic

Table 1 Similarity relation

Parameters	Symbol of similarity coefficient	Calculating formula	Similarity constant
Length	S_l	S_l	1 /8
Strain	1	S_σ/S_E	1
Modulus of elasticity	S_E	$S_E=S_\sigma$	1
Stress	S_σ	S_σ	1
Mass density	S_ρ	S_σ/S_l	8
Mass	S_m	$S_\sigma \cdot S_l^2$	1/64
Vertical force	S_F	$S_\sigma \cdot S_l^2$	1/64

Table 2 The length of plastic hinge

Code	The length of plastic hinge (cm)	Maximum value (cm)
China	15.9	
Caltrans	15.9	
AASHTO	17.2	17.2
Eurocode 8	15.0	
JRA	12.5	

hinge lengths. In addition, some researchers have found that increasing the reinforcement ratio will increase the length of the plastic hinge (Li and Ding 2019). That is, the damage area of the pier becomes longer. In this study, in order to ensure that the damage location of piers is not transferred after increasing the number of longitudinal reinforcement at the bottom of piers, 1.5 times the maximum length of the plastic hinge are adopted.

2.2 Specimen design

A widely used railway bridge pier with rectangular cross section in the earthquake region of China is selected as the prototype in this study. The prototype bridge pier height is 10m, and the size of the cross section is 2.0×2.88 m (width and length). Specimens were designed in accordance with a 1:8 scale of the prototype bridge pier. Detailed scaling similarities are shown in Table 1. Three bridge pier specimens, each with a height of 125 cm and a cross section of 25×36 cm (width and length) were constructed along with a stub of a size of 80×70×50 cm (length, width and height) (Fig. 2). The specimen S1 was designed to have six longitudinal reinforcement bars with 8 mm in diameter in the potential plastic hinge area and four longitudinal reinforcement bars with 8 mm in diameter above the potential plastic hinge area. The increased longitudinal steel bars were bent at the top to ensure that the steel bar and concrete worked together, and the bottom construction of the increased longitudinal steel bars were consistent with the original steel bars construction of the pier (Fig. 2(a)). The specimens S2 and S3, which were used for comparison with the specimen S1, were designed to have 4 and 6 longitudinal reinforcement in all cross sections, respectively (Fig. 2(b) and (c)). The yield strength of longitudinal steel bars with 8 mm in diameter and stirrups with 6 diameters are 335 MPa. The spacing of stirrups is 10.3 cm. Three cubes were tested after 28 days of casting to determine the compressive strength of concrete and their bearing

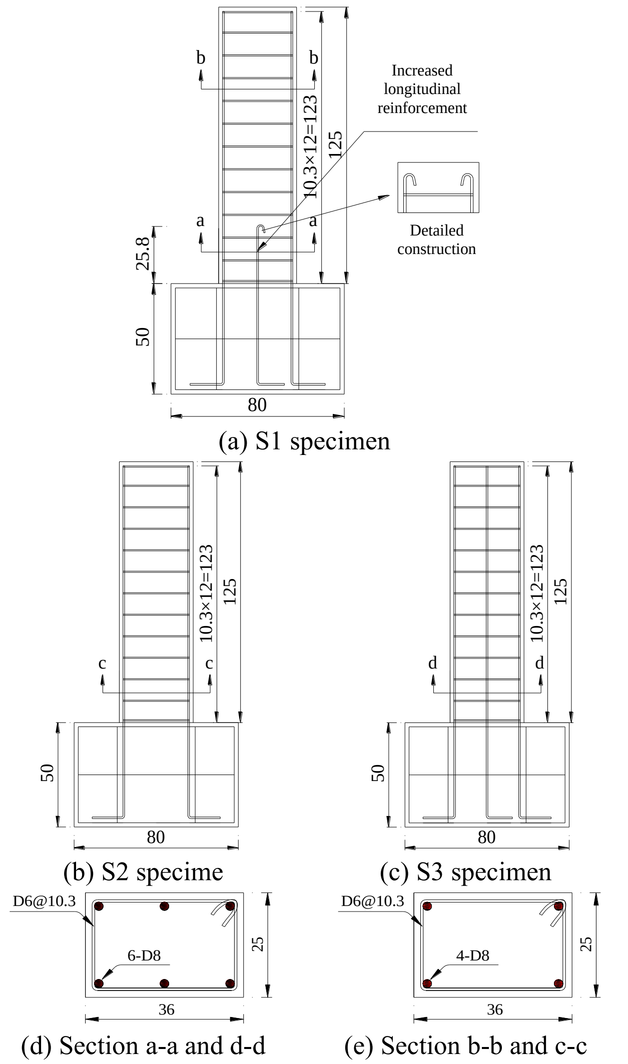

Fig. 2 Size and reinforcement details of specimens S1, S2 and S3 (unit: cm)

platforms was 30 MPa. According to the calculation formula (Eqs. (1) to (5)) of plastic hinge length in Section 2.1, the plastic hinge length values were obtained. As shown in Table 2. The maximum value of the plastic hinge length is 17.2 cm, and 1.5 times of the maximum value is 25.8 cm. Therefore, the height of the increased longitudinal reinforcement at the pier bottom is 25.8 cm in height (Fig. 2 (a)). The detailed parameters of each specimen are shown in Table 3. Size and reinforcement details of each specimen are shown in Fig. 2.

2.3 Specimen formation

According to the three designed specimens, the specimens were made and cured under standard conditions for 28 days. The reinforcement skeletons of three samples are shown in Fig. 3.

3. Test program

3.1 Test equipment

Table 3 Design parameters of bridge pier specimens

ID	Pier height (cm)	Cross-section size (cm)	Axial compression ratio (%)	Longitudinal steel ratio (%)	Diameter of longitudinal steel (mm)	Diameter of hoop steel (mm)
S1	125	36×25	3.96	0.224 (Above the plastic hinge region) 0.335 (In the plastic hinge region)	8	6
S2	125	36×25	3.96	0.224	8	6
S3	125	36×25	3.96	0.335	8	6

(a) Steel bar skeleton of S1

(b)Steel bar skeleton of S2

(c) Steel bar skeleton of S3

Fig. 3 Reinforcement skeletons of three specimens

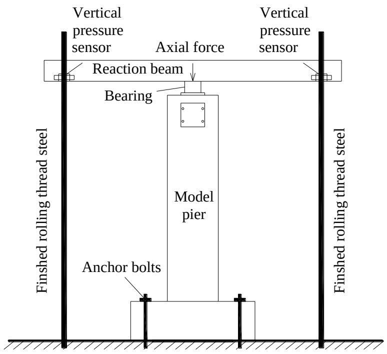

(a) Vertical loading device

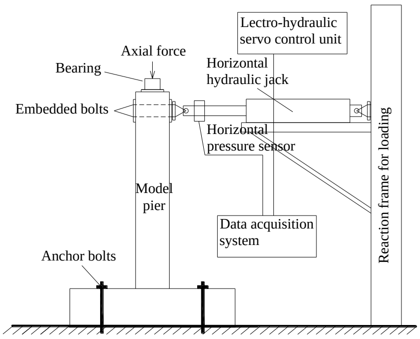

(b) Lateral loading device

Fig. 4 Configuration of the experiment equipment

Fig. 4 shows the loading project of the quasi-static test, in which the cyclic load is applied through the hydraulic jack at the embedded hole on the top of the bridge pier. The maximum load is ±1000 kN and the maximum displacement is ±200 mm. The vertical load was applied through the beam on the top of the pier and 2 pieces of screw-thread steel bar. Pressure sensors were installed between the beam and the screw-thread steel bars to record the applied vertical load. The load was controlled by computer, and the load and displacement on the top of pier were also recorded by computer. The loading device of the test is shown in Fig. 5.

3.2 Displacement measuring points

The main test items are horizontal displacement of pier top and vertical displacement of pier bottom. According to the test content, the measuring point layout of the pier is determined, and a horizontal displacement meter is arranged on the pier top to test the horizontal displacement of the pier top. A vertical displacement meter is arranged on each side of the bottom of the pier in the loading direction to test the displacement caused by bonding slip in the loading process. The detailed arrangement is shown in Fig. 6.

(a) Vertical loading device

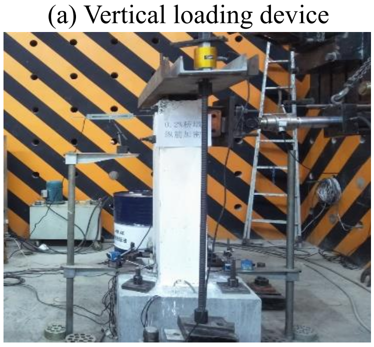

(b) Lateral loading device

Fig. 5 The loading devices of the test

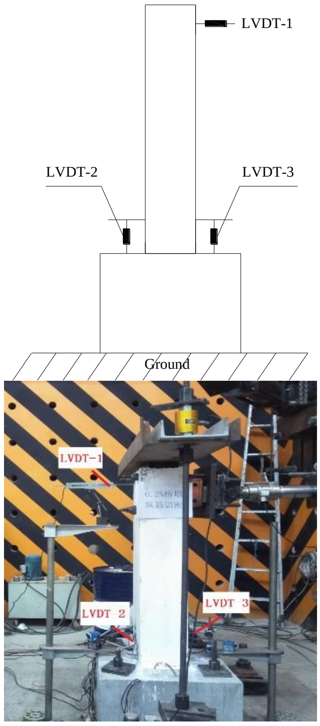

Fig. 6 Displacement measuring point of piers

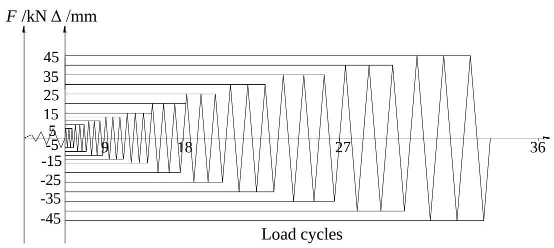

Fig. 7 Lateral cyclic load history

3.3 Lateral load history

The lateral cyclic loading protocol in this study is based on the Specification for seismic test of building in China (China 1997). The force-displacement loading control protocol is adopted for lateral cyclic loading. Force loading control is first used before the pier cracking. After cracking, displacement loading control is adopted, increasing step by step from 5 mm. To be more specific, three cycles at each displacement level is performed; before the displacement of pier top reaches 15 mm, it increases to 2 mm per step, and 5 mm after 15 mm. The rate of the applied displacement is 0.2mm/s in the test. When the horizontal load decreases below 85% of the peak load, it is considered that the pier reaches the ultimate failure state and the loading stops. The detailed lateral load history is shown in Fig. 7.

4. Test results and analysis

4.1 Observations

4.1.1 Specimen S1

When the horizontal force at the top of the pier was increased to 14 kN, cracks appeared at the bottom of the pier, and then displacement loading control method was used. When the horizontal displacement of the pier top was increased to 5 mm, the crack at the bottom of the pier expanded, and a second transverse crack appeared at a distance of 16 cm from the bottom of the pier. When the displacement was increased to 9 mm, the two cracks at the pier bottom and 16 cm away from the pier bottom were connected respectively. With the increase of displacement, the crack opened obviously, but no new crack appeared. When the displacement of the top of the pier was increased to 25 mm, peeling phenomenon appeared on the concrete at the bottom of the pier. With the increase of displacement, the peeling of the concrete was intensified. When the displacement reached 40 mm, the longitudinal steel bar was fractured, and the horizontal load on the pier top decreased below 85% of the peak value, and the pier was destroyed. The final failure state is shown in Fig. 8(a).

4.1.2 Specimen S2

When the horizontal force at the top of the pier was increased to 12 kN, slight cracks appeared locally at the bottom of the pier. When the horizontal force at the top of the pier was increased to 14 kN, growing and expanding cracks appeared, and then displacement loading control method was used. When the horizontal displacement of pier top was increased to 7 mm, the pier bottom crack was penetrated. With the increase of pier top displacement, the crack opened obviously. When the displacement was increased to 25 mm, the second crack appeared about 22 cm above the bottom of the pier and the concrete at the bottom of the pier was partially flaking off. When the displacement of pier top was increased to 30 mm, the second crack was connected around. With the increase of displacement, the peeling of concrete at the bottom of the pier intensified. When the displacement reached 40mm, the longitudinal steel bar was fractured, the concrete at the bottom of the pier was seriously peeling, with horizontal load on the top of the pier dropping below 85% of the peak value, and the bridge pier being destroyed. The final failure state is shown in Fig. 8(b).

4.1.3 Specimen S3

When the horizontal force at the top of the pier was increased to 14 kN, a crack appeared at the bottom of the pier and was 21 cm away from the bottom of the pier, and then displacement loading control method was used. When the horizontal displacement of pier top was increased to 7 mm, the pier bottom crack was connected around. When the displacement was increased to 11 mm, the third crack appeared 40 cm away from the bottom of the pier. When the horizontal displacement of the pier top was increased to 15 mm, the crack 21 cm away from the bottom of the pier was connected along all sides. With the increase of displacement, the crack expansion and the peeling of the concrete at the bottom of the pier intensified, but no new crack appeared. When the displacement reached 45 mm, the longitudinal steel bar was fractured, the concrete at the bottom of the pier was seriously peeling, the horizontal load on the top of the pier dropped below 85% of the peak value, and the bridge pier was destroyed. The final failure state is

(a) Specimen S1 (b) Specimen S2 (c) Specimen S3

Fig. 8 The ultimate failure state of piers

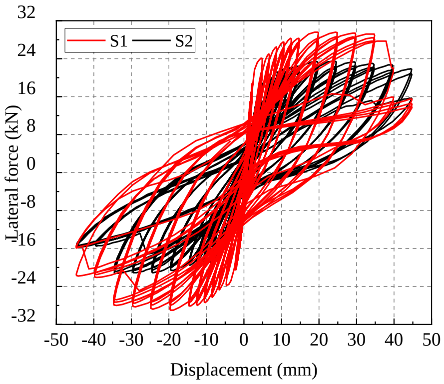

(a) Comparison of specimen S1 and S2

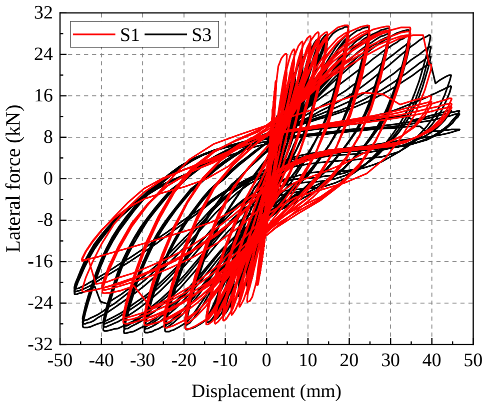

(b) Comparison of specimen S2 and S3

Fig. 9 Hysteresis curves of force-displacement

shown in Fig. 8(c).

4.2 Hysteresis curve

The hysteresis curves of horizontal force and displacement of pier top measured by the test are shown in Fig. 9. As can be seen from Fig. 9(a), the hysteresis loop of specimen S1 is obviously fatter than that of specimen S2, and the maximum bearing capacity is also obviously larger than that of specimen S2, indicating that increased longitudinal reinforcement at the bottom of the pier can significantly improve the bearing capacity and energy dissipation capacity of the pier. As can be seen from Fig. 9(b), the hysteresis curves of specimens S1 and S3 basically coincide before the longitudinal steel bar is pulled, indicating that the seismic performance of the pier with the same reinforcement rate can be basically achieved by improving the reinforcement rate at the bottom of the pier. However, the ultimate displacement decreases slightly.

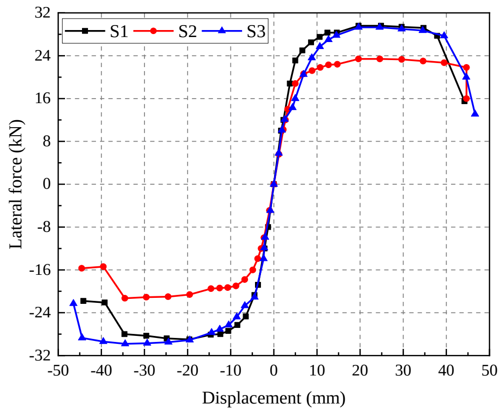

Fig. 10 Skeleton curves of piers

4.3 Skeleton curve

The skeleton curves of the three specimens are shown in Fig. 10. As can be seen from Fig. 10, the horizontal bearing capacity of specimen S2 is obviously lower than that of specimens S1 and S3, and the maximum bearing capacities of specimens S1 and S3 are basically the same, indicating that the bearing capacity of the bridge pier can be significantly increased by only increasing the reinforcement ratio at the bottom of the pier, and it can be increased to a degree basically the same as that of the bridge pier with high reinforcement at the whole pier.

4.4 Stiffness degradation

The stiffness degradation of bridge piers is caused by the cracking of concrete and the yielding of steel bars. It can be seen that the stiffness of the pier decreases with the increase of loading displacement. In order to directly reflect the change of pier stiffness under cyclic load, the concept of secant stiffness is introduced. The specific calculation formula is shown in Eq. (6) (China 1997), where, F_i represents the positive and negative maximum load values under cyclic load of the loading, and Δ_i is the displacement corresponding to the peak load. The stiffness degradation

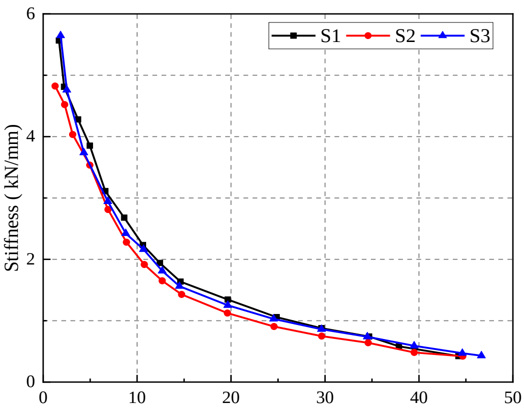

Fig. 11 Stiffness degradation curves of piers

curves of the three specimens are obtained through analysis, as shown in Fig. 11.

$$K_i = \frac{|+F_i| + |-F_i|}{|+\Delta_i| + |-\Delta_i|} \tag{6}$$

As can be seen from Fig. 11, the initial stiffness of specimen S1 is significantly higher than that of specimen S2, and is close to that of specimen S3. With the increase of displacement, the stiffness of the pier decreases continuously. The stiffness of specimen S1 is always higher than that of specimen S2, and is close to that of specimen S3, indicating that increasing the reinforcement ratio at the bottom of the pier can improve the stiffness of the pier.

4.5 Displacement ductility coefficient

According to the skeleton curve, the Park method (Park 1989) is used to estimate the yield displacement and ultimate displacement of the bridge pier, as shown in Fig. 12. Specific steps are as follows: on the basis of the skeleton curve, determine the maximum lateral force $F_{\max}$ and point A of 0.75 $F_{\max}$ on the skeleton curve. Connect the origin to A and extend the line to the horizontal line of maximum lateral force at point B, the displacement corresponding to the intersection point is the yield displacement Δ_y, and the displacement corresponding to 0.85 $F_{\max}$ in the descending section of the skeleton curve is the limit displacement Δ_u. Then the displacement extension coefficient can be expressed as

$$\mu = \Delta_u / \Delta_y \tag{7}$$

The yield displacement, limit displacement and displacement ductility coefficients of each pier are listed in Table 4. It can be seen from the calculation results that the yield displacement of specimen S1 is between specimen S2 and S3, which is improved, compared with specimen S2. The ultimate displacements of specimens S1 and S2 are basically the same, both smaller than that of specimen S3, indicating that only increasing the reinforcement ratio at the bottom of the bridge pier can improve the yield displacement of the bridge pier, but have little influence on the ultimate displacement. The displacement ductility coefficient of specimen S1 is between specimen S2 and S3, indicating that the displacement ductility coefficient decreases slightly with the increase of reinforcement ratio.

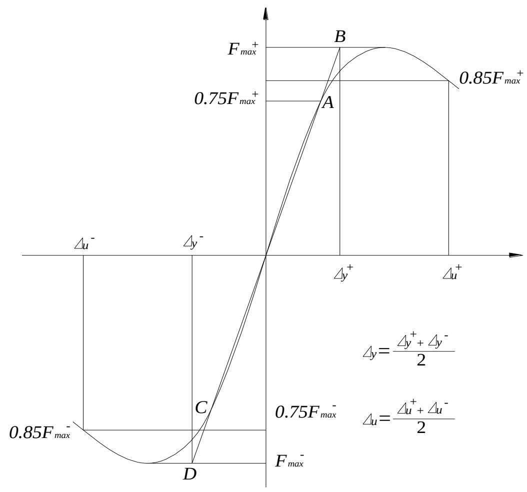

Fig. 12 Schematic diagram of yield displacement calculation

Table 4 Displacement ductility coefficient calculation

ID	Yield displacement (mm)	Limit displacement (mm)	Displacement Ductility coefficient	Average displacement ductility coefficient
S1	7.94	41.04	5.17	5.02
	-7.78	-37.84	4.86	
S2	6.02	44.66	7.42	6.65
	-6.48	-37.50	5.88	
S3	10.39	41.81	4.02	4.87
	8.31	-47.50	5.72	

4.6 Energy-dissipating capacity

The energy dissipation capacity of a bridge pier is the ability to absorb energy due to plastic deformation under the action of seismic force, and it is also an important index to evaluate the seismic performance of the bridge pier. In engineering seismic design, cumulative energy consumption is generally used to quantitatively assess the energy dissipation capacity of bridge piers (Tian *et al.* 2017). According to the calculation method in literature (Wang *et al.* 2018), the curve of accumulated energy dissipation of each pier changing with displacement is obtained, as shown in Fig. 13.

It can be seen from Fig. 13 that the total cumulative energy consumption of specimen S1 is significantly higher than that of specimen S2, and the cumulative energy consumptions of specimen S1 and S3 are basically the same, and the cumulative energy consumption of specimen S1 under the same displacement is also significantly higher than that of specimen S2, indicating that only increasing the reinforcement ratio at the bottom of the pier can also increase the energy consumption of the pier, and can reach almost the same level as the cumulative energy consumption of the pier with high reinforcement in the whole pier.

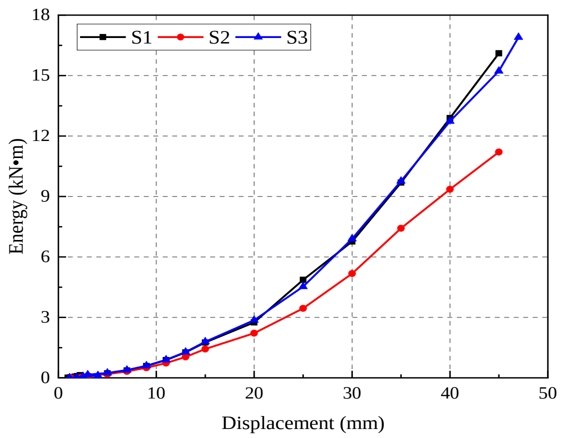

Fig. 13 Cumulative energy consumption curve of bridge piers

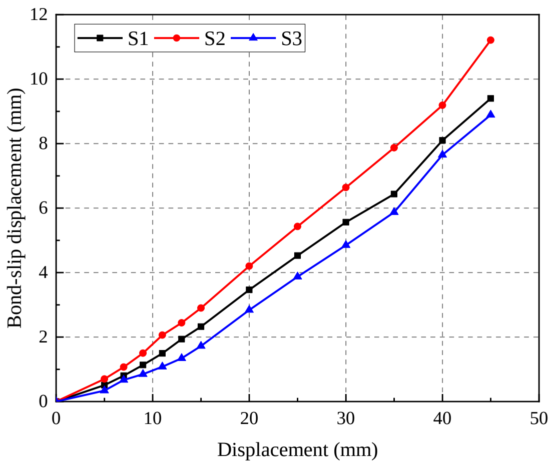

Fig. 14 Slippage displacement between steel bar and concrete

4.7 Bond-slip displacement between reinforcing bar and concrete

A longitudinal reinforcement embedded in concrete under tension will accumulate strain over the embedment length of the steel bar. This strain causes the longitudinal reinforcement to slip, or extend, relative to the concrete in which it is embedded (Sezen and Setzler 2008, Lin and Zhang 2013, Gooranorimi *et al.* 2017, Mousavi *et al.* 2019). The bond-slip between reinforcing bar and concrete is reflected in the width of cracks in the footing or pier and pile cap joint zone. In this study, the displacement of pier bottom lifting is measured by LVDT-2 and LVDT-3. With the increase of pier top displacement, the value of bond-slip is shown in Fig. 14.

As can be seen from Fig. 14, the bond-slip displacement of specimen S1 is obviously smaller than that of specimen S2, indicating that the bond-slip between reinforcing bar and concrete can be reduced by adding short longitudinal reinforcement in the plastic hinge zone of pier bottom. The bond-slip displacement of specimen S1 is larger than that of specimen S3, indicating that the longitudinal reinforcement above the plastic hinge zone has an effect on the bond-slip displacement between reinforcing bar and concrete.

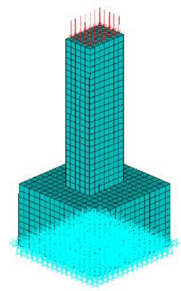

Fig. 15 The finite element model

5. Numerical simulation analysis

5.1 Finite element model

In order to conduct further numerical simulation analysis, a numerical model of the piers was developed by the finite element software ANSYS. In the numerical model, Mander constitutive model (Mander and Priestley 1988) was adopted to simulate the cyclic behavior of the concrete material; KINH model (Dodd and Restrepo-Posada 1995) that could reflect the bauschinger effect of the reinforcing steel implemented in ANSYS was used to simulate the reinforcing bars. In addition, the modeling method that a unit was established between the steel bar node and the concrete node was used to analyze the effect of bond-slip between reinforcement and concrete on the shape of bridge pier hysteresis curves. The rational elastic model (Han *et al.* 2003) was applied to simulate the bond-slip between steel bar and concrete. In the finite element model, the element SOLID65 was adopted to simulate concrete, and the element LINK180 and the element COMBIN39 in ANSYS were used to simulate steel bar and the bond-slip relationship between reinforcement and concrete, respectively. Considering the accuracy of results, the element mesh size was about 50 mm×50 mm×50 mm. The vertical force was applied using area load, which was converted according to the actual load value in the tests. In the finite element model, the nodes at the bottom of the cushion cap were fixed. The finite element model was shown in Fig. 15.

5.2 Comparison of numerical and experimental results

In order to verify the accuracy of the above numerical modeling method, the hysteretic curves of the finite element model are compared with the experimental results, as shown in Fig. 16. It can be found that the hysteretic curves obtained from numerical simulation agree well with those of the experimental results, and the hysteretic behavior of the specimens is accurately reproduced, which verifies the accuracy of the given finite element analysis model.

5.3 Numerical analysis of piers with different numbers of longitudinal reinforcement

In order to further analyze the influence of increasing the number of longitudinal steel bar in plastic hinge area on

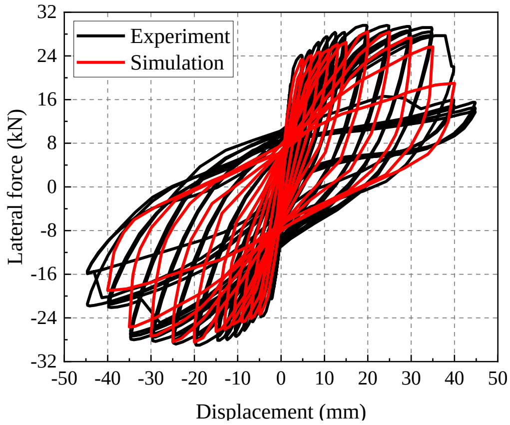

(a) Comparison of specimen S1

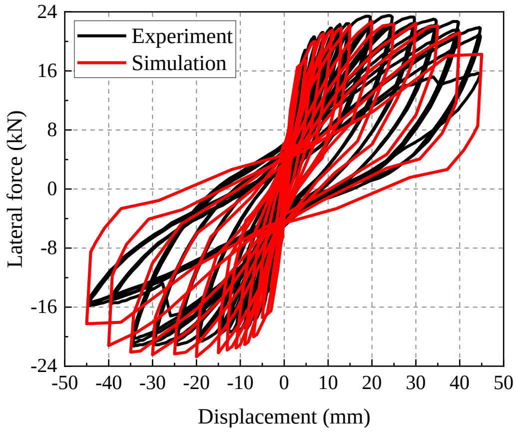

(b) Comparison of specimen S2

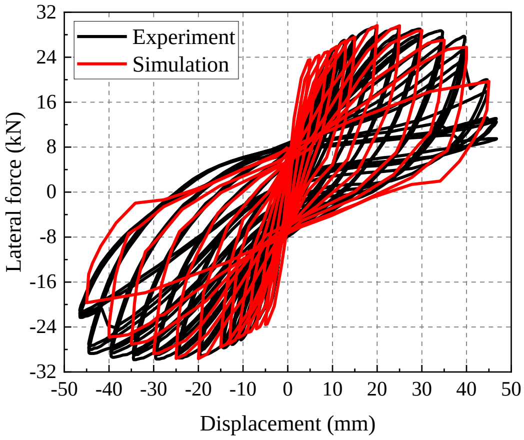

(c) Comparison of specimen S3

Fig. 16 Comparison of hysteretic curves

Table 5 Design parameters of longitudinal reinforcement

ID	Longitudinal steel ratio (%)	Proportion of increase (%)
M1	0.34 (Above the plastic hinge region) 0.56 (In the plastic hinge region)	65
M2	0.56	-
M3	0.45 (Above the plastic hinge region) 0.67 (In the plastic hinge region)	49
M4	0.67	-

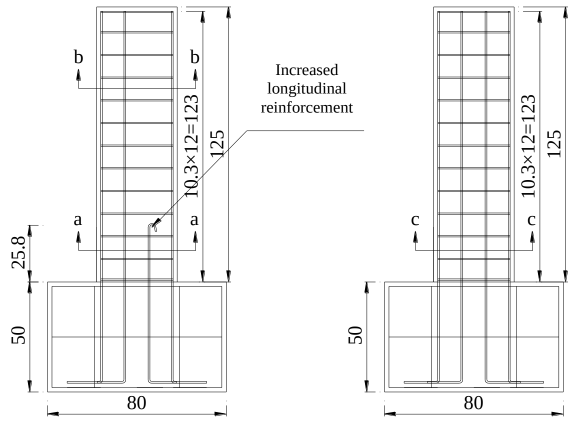

(a) M1 specimen (b) M2 specimen

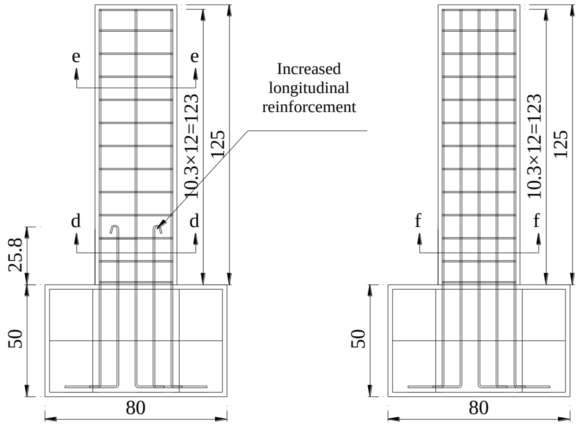

(c) M3 specimen (d) M4 specimen

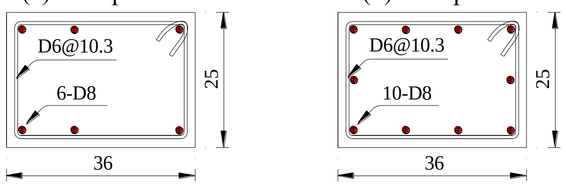

(e) section b-b (f) section a-a and c-c

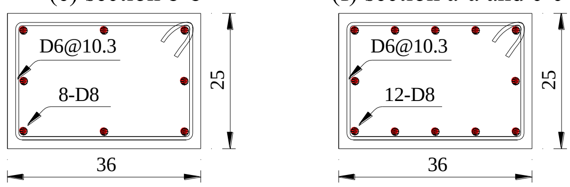

(g) section d-d (h)section e-e and f-f

Fig. 17 Comparison of hysteretic curves

the seismic performance of piers, piers with different longitudinal reinforcement ratios are analyzed based on the above numerical analysis model. The height, cross-section size, stirrup ratio and steel bar diameter of the piers are the same as those of three specimens. Design parameters of longitudinal reinforcement are listed in Table 5. The longitudinal steel bar quantity and layout spacing of the piers are shown in Fig. 17. The hysteretic curves and skeleton curves of the piers are obtained from numerical simulation, as shown in Fig. 18 and Fig. 19.

As can be seen from Fig. 18, the hysteretic curves of M1 pier and M2 pier (M3 pier and M4 pier) basically coincide. However, when the loading displacement is more than 45 mm, the shape of the hysteretic curve of M1 pier (M3 pier) is thinner than that of M2 pier (M4 pier). Because the number of longitudinal steel bars above the plastic hinge

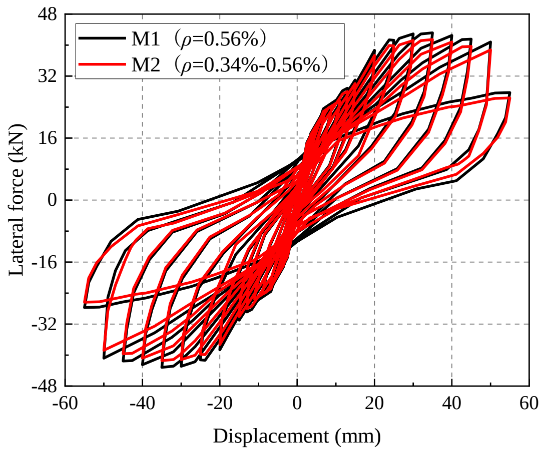

(a) Comparison of M1and M2

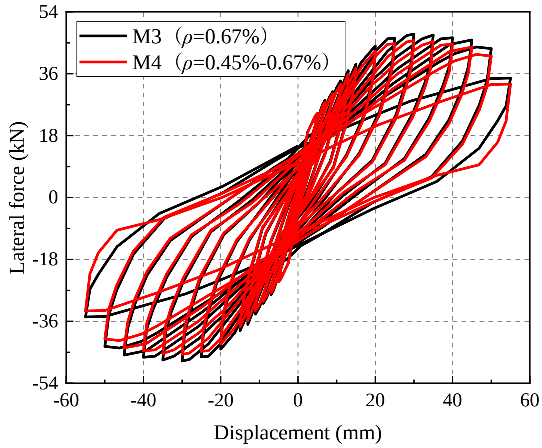

Comparison of M3 and M4

Fig. 18 Comparison of hysteretic curves

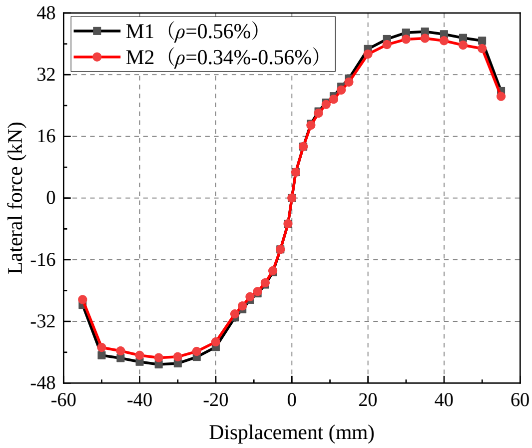

(a) Comparison of M1and M2

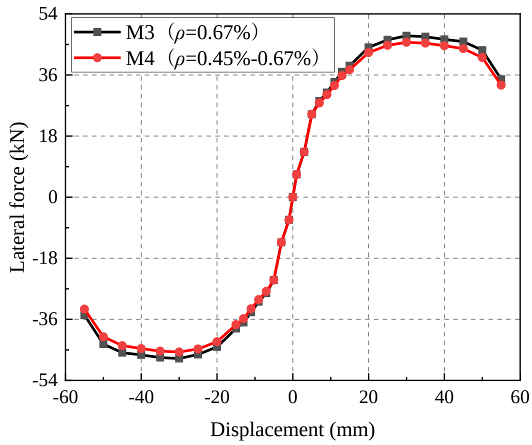

(b) Comparison of M3 and M4

Fig. 19 Comparison of skeleton curves

area of M1 pier and M3 pier is fewer than those of M2 pier and M4 pier, respectively, so that there is a large bond-slip between steel bar and concrete. As can be seen from Fig. 19, the skeleton curve of M1 pier (M3 pier) and M2 pier (M4 pier) is in good agreement. In the elastic stage, the skeleton curves of M1 pier and M2 pier (M3 pier and M4 pier) coincide completely. In the elastic-plastic stage, the peak load of M1 pier can reach 0.96 times that of M2 pier, and the peak load of M3 pier can reach 0.95 times that of M4 pier. In general terms, the seismic performance of piers with only increasing the number of reinforcing bars (less than 65%) in the plastic hinge zone at the bottom of piers can be basically equivalent to that of piers whose number of reinforcing bars in all sections is the same as that in plastic hinge zone.

6. Conclusions

Based on the failure characteristics of piers with bending failure in earthquake, a new arrangement method of longitudinal reinforcement for railway bridge pier is proposed in this study. It is believed that this effort might provide guidance for railway bridge designers. Quasi-static test of three scaled models have been carried out to investigate their seismic performance, and the following conclusions can be drawn from this study:

• From the failure characteristics, it can be found from the ultimate failure state of the three model piers that when the longitudinal reinforcement bar is ruptured, the concrete at the bottom of the pier is crushed. This indicates that the failure characteristics of the pier with increasing an appropriate amount of longitudinal reinforcement in the bottom plastic hinge area are not changed and the vulnerable position is not transferred.

• From the hysteresis curves and the skeleton curves, it can be found that increasing the number of longitudinal reinforcement in the plastic hinge area not only makes the hysteresis curve of the pier fuller, but also improves the lateral bearing capacity of the pier.

• Based on the analysis of the seismic performance parameters of the three specimens, it can be found that increasing the number of longitudinal steel bars in plastic hinge area can obviously improve energy dissipation capacity of piers, increase the initial stiffness of the pier and reduce the bond-slip displacement between steel bar and concrete.

• According to both the experimental results and numerical simulation results, it can be found that the seismic performance of piers with only increasing the number of steel bars (less than 65%) in the plastic hinge zone can be basically equivalent to that of piers whose number of steel bars in all sections is the same as that in plastic hinge zone.

This method of increasing appropriate amount of longitudinal reinforcement in plastic hinge area to improve seismic performance of bridge piers is feasible and verified by quasi-static test.

Acknowledgements

This work was supported by the National Natural Science Foundation of China (Grant No. 51768036), and National Natural Science Foundation of China for Young Scholar (Grant No. 51808273).

Disclosure statement

No potential conflict of interest was reported by the authors.

References

Aashto (1995), Standard Specifications for Highway Bridges 16 Edition, Washington, American Association of State Highway and Transportation Officials (AASHTO), Inc.

Aboutaha, R.S., Engelhardt, M.D., Jirsa, J.O. and Kreger, M.E. (1996), "Retrofit of concrete columns with inadequate lap splices by the use of rectangular steel jackets", *Earthq. Spectra*, **12**(4), 693-714.

Aboutaha, R.S., Engelhardt, M.D., Jirsa, J.O. and Kreger, M.E. (1999), "Experimental investigation of seismic repair of lap splice failures in damaged concrete columns", *ACI Struct. J.*, **96**(2), 57-67.

Abdelnaby, A.E., Frankie, T.M., Elnashai, A.S., Spencer, B.F., Kuchma, D.A., Silva, P. and Chang, C.M. (2014), "Numerical and hybrid analysis of a curved bridge and methods of numerical model calibration", *Eng. Struct.*, **70**, 234-245. https://doi.org/10.1016/j.engstruct.2014.04.009.

Association, J.R. (1996), *Road and Bridge Display Book, Seismic Design Chapter:V*, Japan Road Association, Tokyo.

Bruneau, M., Wilson, J.C. and Tremblay, R. (1996), "Performance of steel bridges during the 1995 Hyogo-ken Nanbu (Kobe, Japan) earthquake", *Can. J. Civil Eng.*, **23**(3), 678-713. https://doi.org/10.1139/l96-883.

Caltrans (2006), *Caltrans Seismic Design Criteria Version 14*, Caltrans, Sacramento.

CEN (European Committee for Standardization) (2005), Design of Structures for Earthquake Resistance, Part 2: Bridges, Eurocode 8, BS EN 1998-2.

China (2008), Guidelines for seismic design of highway bridges.

Ding, M., Chen, X., Zhang, X., Liu, Z. and Lu, J. (2018), "Study on seismic strengthening of railway bridge pier with cfrp and concrete jackets", *Earthq. Struct.*, **15**(3), 275-283. https://doi.org/10.12989/eas.2018.15.3.275.

Dodd, L.L. and Restrepo-Posada, J.I. (1995), "Model of predicting cyclic behavior of reinforcing steel", *J. Struct. Eng.,* ASCE, **121**(3), 433-445. https://doi.org/10.1061/(ASCE)0733-9445(1995)121:3(433).

Ghosh, K.K. and Sheikh, S.A. (2007), "Seismic upgrade with carbon fiber-reinforced polymer of columns containing lap-spliced reinforcing bars", *ACI Struct. J.*, **104**(2), 227-236.

Gooranorimi, O., Suaris, W. and Nanni, A. (2017). "A model for the bond-slip of a gfrp bar in concrete", *Eng. Struct.*, **146**, 34-42. https://doi.org/10.1016/j.engstruct.2017.05.034.

Hall, J.F. (1995), "Northridge earthquake of January 17, 1994: Reconnaissance report, volume 1-highway bridges and traffic management", *Earthq. Spectra*, **11**(3), 287-372.

Han, T.S., Feenstra, P.H. and Billington, S.L. (2003), "Simulation of highly ductile fiber-reinforced cement-based composite components under cyclic loading", *ACI Struct. J.*, **100**(6), 749-757.

Harries, K., Ricles, J., Pissiki, S. and Sause, R. (2006), "Seismic retrofit of lap splices in nonductile columns using cfrp jackets", *ACI Struct. J.*, **103**(6), 226-236.

Iacobucci, R.D., Sheikh, S.A. and Bayrak, O. (2003), "Retrofit of square concrete columns with carbon fiber-reinforced polymer for seismic resistance", *ACI Struct. J.*, **100**(6), 785-794.

Iwasaki, K., Hagiwara, T., Koyama, H. and Yoshaida, T. (1985), "Experimental investigation on hysteretic behavior of reinforced concrete columns", *Proceedings of the Second Joint U.S. -Japan Workshop on Performance and Strengthening of Bridge Structures and Research Needs*, San Francisco, CA.

Jaradat, O.A., Mclean, D.I. and Marsh, M.L. (1998), "Performance of existing bridge columns under cyclic loading-part 1 experimental results and observed behavior", *ACI Struct. J.*, **95**(6), 695-704.

Jaradat, O.A., Mclean, D.I. and Marsh, M.L. (1999), "Performance of existing bridge columns under cyclic loading-part 2: Analysis and comparisons with theory", *ACI Struct. J.*, **96**(1), 57-67.

JGJ 101-96 (1997), Specification of Testing Methods for Earthquake Resistant Building.

Jennings, P.C. (1971), "Engineering features of the san fernando earthquake of february 9", Earthquake Engineering Research Laboratory, California Institute of Technology, Pasadena.

Jia, J., Song, N., Xu, Z., He, Z. and Bai, Y. (2015), "Structural damage distribution induced by wenchuan earthquake on 12th may, 2008", *Earthq. Struct.*, **9**(1), 93-109. https://doi.org/10.12989/eas.2015.9.1.093.

Jiang, L., Shao, G., Jiang, J. and Wang, H. (2013), "Experimental study on seismic performance of solid piers with round ended cross-section in high-speed railway", *China Civil Eng. J.*, **46**(3), 86-95.

Kunnath, S.K., El-Bahy, A., Taylor, A. and Stone, W. (1997), "Cumulative seismic damage of reinforced concrete bridge piers", Department of Commerce, Washington, USA.

Kuochun, C., Dyiwei, C., Menghao, T. and Yuchi, S. (2000), "Seismic performance of highway bridges", *Earthq. Eng. Eng. Seismol.*, **2**(1), 55-77. https://doi.org/10.1016/0141-0296(88)90002-8.

Lee, C.S. and Han, S.W. (2019), "Cyclic behaviour of lightly-reinforced concrete columns with short lap splices subjected to unidirectional and bidirectional loadings", *Eng. Struct.*, **189**, 373-384. https://doi.org/10.1016/j.engstruct.2019.03.108.

Lehman, D., Moehle, J. and Mahin, S. (2004), "Experimental evaluation of the seismic performance of reinforced concrete bridge columns", *J. Struct. Eng.*, **130**(6), 869-879. https://doi.org/10.1061/(ASCE)0733-9445(2004)130:6(869).

Li, J. and Ding, M. (2019), "Shaking table test of reinforced concrete pier with longitudinal reinforcement encrypt in plastic hinge area", *J. Railw. Sci. Eng.*, **16**(7), 1-7.

Lin, X. and Zhang, Y.X. (2013), "Bond-slip behaviour of frp-reinforced concrete beams", *Constr. Build. Mater.*, **44**(3), 110-117. https://doi.org/10.1016/j.conbuildmat.2013.03.023.

Mander, J.B., Mahmoodzadegan, B., Bhadra, S. and Chen, S.S. (1996), "Seismic evaluation of a 30-year old non-ductile highway bridge pier and its retrofit", Department of Commerce, Washington.

Mander, J.B., Priestley, M.J. and Park, R. (1988), "Theoretical stress-strain modal for confined concrete", *J. Struct. Eng.*, **114**(8), 1804-1826. https://doi.org/10.1061/(ASCE)0733-

9445(1988)114:8(1804).

Meli, R., Baeza, J. and Rodrigue, M. (1984), "Hysteretic behavior of concrete flexural members with high strength steel", *Eighth World Conferece on Earthquake Engineering*.

Mergos, P.E. and Kappos, A.J. (2015), "Estimating fixed-end rotations of reinforced concrete members at yielding and ultimate", *Struct. Concrete*, **16**(4), 537-545. https://doi.org/10.1002/suco.201400067.

Mousavi, S.S., Guizani, L. and Ouellet-Plamondon, C.M. (2019), "On bond-slip response and development length of steel bars in pre-cracked concrete", *Constr. Build. Mater.*, **199**, 560-573. https://doi.org/10.1016/j.conbuildmat.2018.12.039.

Ni, S.D., Wang, W.T. and Li, L. (2010), "The april 14th, 2010 yushu earthquake, a devastating earthquake with foreshocks", *Sci. China Earth Sci.*, **53**(6), 791-793.

Ohno, T. and Nishioka, T. (1984), "An experimental study on energy absorption capacity of columns in reinforced concrete structures", *Doboku Gakkai Ronbunshu*, **1984**(350), 23-33. https://doi.org/10.2208/jscej.1984.350_23.

Park, R. (1989), "Evaluation of ductility of structures and structural assemblages from laboratory testing", *Bull. NZ Nat. Soc. Earthq. Eng.*, **22**(3), 155-166.

Priestley, M.J.N. and Benzoni, G. (1996), "Seismic performance of circular columns with low longitudinal reinforcement ratios", *ACI Struct. J.*, **93**(4), 474-485.

Rajput, A.S. and Sharma, U.K. (2018), "Seismic behavior of under confined square reinforced concrete columns", *Struct.*, **13**, 26-35. https://doi.org/10.1016/j.istruc.2017.10.005.

Sezen, H. and Setzler, E.J. (2008), "Reinforcement slip in reinforced concrete columns", *ACI Struct. J.*, **105**(3), 280-289.

Su, J., Dhakal, R.P., Wang, J. and Wang, W. (2017), "Seismic performance of rc bridge piers reinforced with varying yield strength steel", *Earthq. Struct.*, **12**(1), 201-211. https://doi.org/10.12989/eas.2017.12.2.201.

Sun, Z. (2012). "Research on the seismic deformation capacity of RC bridge columns", Ph.D., China Earthquake Administration.

Tanaka, H. (1990), "Effect of lateral confining reinforcement on the ductile behavior of reinforced concrete columns", University of Canterbury, Christchurch.

Tehrani, P. and Mitchell, D. (2013), "Effects of column stiffness irregularity on the seismic response of bridges in the longitudinal direction", *Can. J. Civil Eng.*, **40**(8), 815-825. https://doi.org/10.1139/cjce-2012-0091.

Tian, T., Qiu, W., Qi, Z. and Zhang, Z. (2017), "Experimental study for effects of shear span ratio on seismic proformance of concrete filled steel tube (cfst) composite bridge columns", *J. Dalian Univ. Technol.*, **57**(2), 133-141.

Valluvan, R., Kreger, M.E. and Jirsa, J.O. (1993), "Strengthening of column splices for seismic retrofit of nonductile reinforced concrete frames", *ACI Struct. J.*, **90**(4), 432-440.

Wang, W., Li, Z., Dang, H. and Shi, W. (2017), "Strong motion records and its characteristics in jiuzhaigou ms 7.0 earthquake on august 8,2017", *Eng. J.*, **39**(4), 652-656.

Wang, Z., Qu, H. and Li, T. (2018), "Quasi-static cyclic tests of precast bridge columns with different connection details for high seismic zones", *Eng. Struct.*, **158**, 13-27. https://doi.org/10.1016/j.engstruct.2017.12.035.

Wehbe, N.I., Saiidi, M.S. and Sanders, D.H. (1999), "Seismic performance of rectangular bridge columns with moderate confinement", *ACI Struct. J.*, **96**(2), 248-258.

Xiao, J. and Zhang, C. (2008), "Seismic behavior of RC columns with circular, square and diamond sections", *Constr. Build. Mater.*, **22**(5), 801-810. https://doi.org/10.1016/j.conbuildmat.2007.01.010.

Xue, J., Zhou, C., Liu, Z. and Qi, L. (2018), "Seismic response of steel reinforced concrete spatial frame with irregular section columns under earthquake excitation", *Earthq. Struct.*, **14**(4), 337-347. https://doi.org/10.12989/eas.2018.14.4.337.

Zhao, G., Zhang, T. and Chen, X. (2014), "Experimental study on the seismic performance of high speed railway bridge pier under low cyclic loading", *China Railw. Sci.*, **35**(4), 38-44.

CC